

Optimal constant piecewise vaccination and lockdown policies for COVID-19

Gabriel A. Salcedo-Varela^a, F. Peñuñuri^b, D. González-Sánchez^c, Saúl Díaz-Infante^{c,*}

^a Departamento de Matemáticas, Universidad de Sonora, Blvd. Luis Encinas y Rosales S/N, Hermosillo, Sonora, México, C.P. 83000.

^b Facultad de Ingeniería, Universidad Autónoma de Yucatán, A.P. 150, Cordemex, Mérida, Yucatán, México.

^c CONACYT-Universidad de Sonora, Departamento de Matemáticas, Blvd. Luis Encinas y Rosales S/N, Hermosillo, Sonora, México, C.P. 83000.

Abstract

We formulate a controlled system of ordinary differential equations, with vaccination and lockdown interventions as controls, to simulate the mitigation of COVID-19. The performance of the controls is measured through a cost functional involving vaccination and lockdown costs as well as the burden of COVID19 quantified in DALYs. We calibrate parameters with data from Mexico City and Valle de Mexico. By using differential evolution, we minimize the cost functional subject to the controlled system and find optimal policies that are constant in time intervals of a given size. The main advantage of these policies relies on its practical implementation since the health authority has to make only a finite number of different decisions. Our methodology to find optimal policies is relatively general, allowing changes in the dynamics, the cost functional, or the frequency the policymaker changes actions.

Keywords: COVID-19, Optimal Control, Vaccination, lockdown, DALYs.

1. Introduction

At the date of writing this manuscript, the USA is running its COVID-19 vaccination with Pfizer-BioNTech vaccine. This vaccine development along with Astra-Zeneca, Cansino, Sputnik V, Novavax among others' promise to deliver enough doses for Latin America. In Mexico, particularly, the first stock with around 40 000 shots has arrived past Christmas. In past October, WHO established a recommended protocol for prioritizing access to this pharmaceutical hope giving clear lines about who has to be vaccinated first and why. However, each developed vaccine implies different issues around its application. For example, Pfizer-BioNTech vaccine requires two doses and particular logistics requirements that demand special services. Mexico, despite Pfizer-BioNTech has been taking the responsibility to capacitate personnel that manage the vaccination, there is an explicit demand for logistics resources that limit the institutions' response. On the hand, nonpharmaceutical interventions (NPIs), like a lockdown, also involve economic costs. Our research in this manuscript explores the effect of two interventions, vaccination and lockdown, to mitigate the propagation of COVID-19.

Among the related literature about the two interventions we deal with in this paper, we can mention the following. The problem of who is vaccinated first, when the number of available shots is limited, has been transformed into an optimal allocation problem of vaccine doses in [1, 2]. These articles give answers to the critical question of how much doses allocate to each different group according to risk and age to minimize the burden of COVID-19. In our study, we take the allocation for granted and consider only the vaccination rate.

*Corresponding author

Email addresses: a211203745@unison.mx (Gabriel A. Salcedo-Varela), francisco.pa@correo.uady.mx (F. Peñuñuri), dgonzalezsa@conacyt.mx (D. González-Sánchez), saul.diazinfante@unison.mx (Saúl Díaz-Infante)

Further, papers modeling NPIs consider the diminish of contact rates—by reducing mobility—or modulating parameters regarding the generation of new infections by linear controls [3, 4], Lockdown–Quarantine [5], shield immunity [6]. In addition, Libotte et. al. reports in [7] optimal vaccination strategies for COVID-19.

Since health services’ response will be limited by the vaccine stock and logistics costs, implementing in parallel NPIs is imminent. We focus on formulating and studying via simulation a Lockdown–Vaccination system by consider the vaccine recently approved by Mexico Health Council. We aim to design a schedule for dose application subject to a given vaccine stock that will be applied in a given period of time. For this purpose, we formulate an optimal control problem that minimizes the burden of COVID-19 in DALYs [8], the cost generated by running the vaccination campaign, and economic damages due to lockdown.

One of the main features of our model is that we consider piecewise constant control policies instead of general measurable control policies —also called permanent controls—to minimize a cost functional. General control policies are difficult to implement since the authority has to make different choices every permanently. The optimal policies we find are constant in each interval of time and hence these policies are easier to implement. To the best of our knowledge, our manuscript is the first optimal control model with both lockdown and vaccination strategies that are easy to implement in the sense described above.

In Section 2, we formulate the basic spread model for COVID19 and calibrate its parameters. Then, Section 3 establishes the lockdown–vaccination model and discusses the regarding reproductive number in Section 4. In Section 5 we describe the optimal control problem which consists in minimizing a cost functional subject to controlled lockdown–vaccination system. The optimal policies we find, by solving numerically the optimal control problem, are presented in Section 6. We conclude with some final comments in Section 7.

2. Covid-19 spread dynamics

We split a given population of size N in the basic SEIR structure with segregated classes according to the manifestation of symptoms. Let $L, S, E, I_S, I_A, H, R, D$ respectively denote the class of individuals according to their current state, namely

Lockdown (L) All individuals that have low or null mobility and remain under isolation. Thus individuals in this class reduce their contagion probability.

Suceptible (S) Individuals under risk

Exposed (E) Population fraction that hosts SARS-CoV-2 but cannot infect

Infected-Symptomatic (I_S) Population infected fraction with symptoms and reported as confirmed cases

Infected-Asymptomatic (I_A) Infected individuals with transitory or null symptoms and unreported

Hospitalized (H) Infected population that requires hospitalization or intensive care.

Recover or removed (R) Population that recovers from infection and develops partial immunity

Death (D) Population fraction that died due to COVID-19

To fit data of cumulative reported symptomatic cases, we postulate the counter state Y_{I_S} and make the following assumptions.

Assumptions 1. According to above compartment description, we made the following hypotheses.

(A-1) We suppose that at least 30 % of the population is locked down and a fraction of this class eventually moves to the susceptible compartment at rate δ_L .

(A-2) Force infection is defined as the probability of acquiring COVID-19 given the contact with a symptomatic or asymptomatic individual. Thus we normalize with respect to alive population N^* .

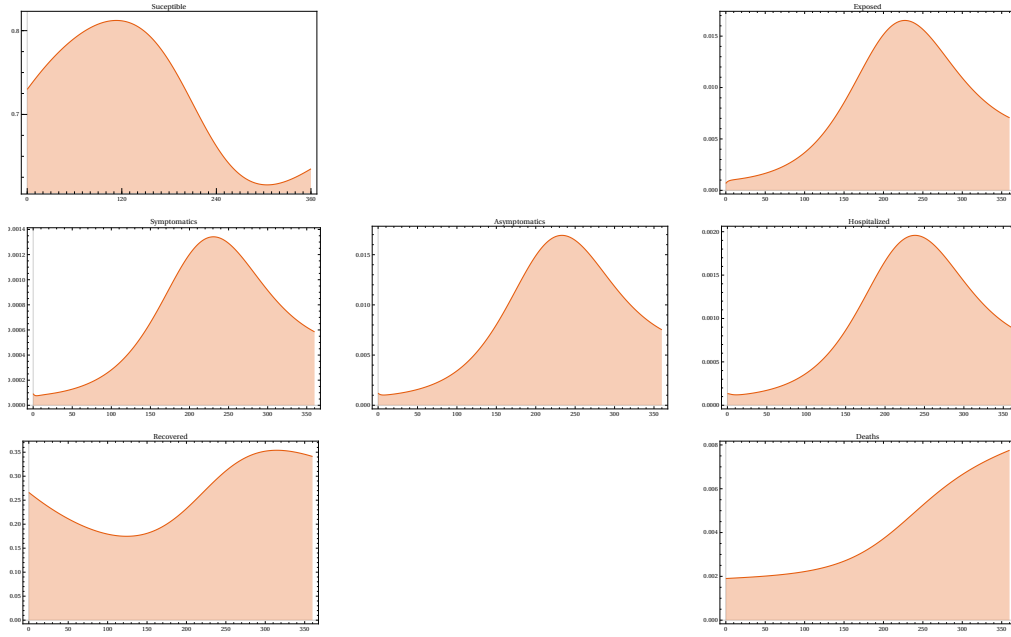


Figure 1: Spread dynamics of COVID-19 according to model in Equation (1).

(A-3) Susceptible individuals become exposed—but not infectious—when they are in contact with asymptomatic or symptomatic individuals. Thus β_S and β_A denote the probabilities of being infectious given the contact with a symptomatic or asymptomatic infectious individuals, respectively.

(A-4) After a period of latency $1/\kappa = 5.1$ days, an exposed individual becomes infected. Being p the probability of developing symptoms and $(1 - p)$ the probability of becoming infectious but asymptomatic. Thus $p\kappa E$ denotes the exposed individuals that become infectious and develop symptoms.

(A-5) Asymptomatic individuals do not die or stay in the Hospital.

(A-6) A fraction μ_H of symptomatic individuals dies due to COVID-19 without hospitalization.

Thus we formulate the following Ordinary Differential Equation (ODE)

$$\begin{aligned}
 S' &= \mu N^* + \delta_R R - (\lambda + \mu) S, \\
 E' &= \lambda(\epsilon L + S) - (\kappa + \mu) E, \\
 I_S' &= p\kappa E - (\gamma_S + \delta_H + \mu_{I_S} + \mu) I_S, \\
 I_A' &= (1 - p)\kappa E - (\gamma_A + \mu) I_A, \\
 H' &= \delta_H I_S - (\gamma_H + \mu_H + \mu) H, \\
 R' &= \gamma_S I_S + \gamma_A I_A + \gamma_H H - (\delta_R + \mu) R, \\
 D' &= \mu_{I_S} I_S + \mu_H H, \\
 \frac{dY_{I_S}}{dt} &= p\kappa E, \\
 \lambda &:= \frac{\beta_A I_A + \beta_S I_S}{N^*}, \\
 N^*(t) &= L + S + E + I_S + I_A + H + R.
 \end{aligned} \tag{1}$$

See Table 1 for notation and references values. [Put here the flow diagram](#)

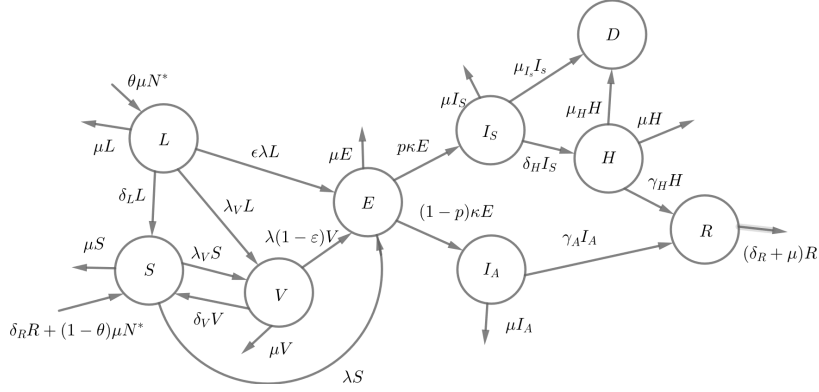


Figure 2: Flow diagram of equation (1)

Parameter	Description
μ	Death rate
β_S	Infection rate between susceptible and symptomatic infected
β_A	Infection rate between susceptible and asymptomatic infected
λ_V	Vaccination rate
δ_V^{-1}	Vaccine-induced immunity
ε	Vaccine efficacy
κ^{-1}	Average incubation time
p	New asymptomatic generation proportion
θ	Proportion of susceptible individuals under lockdown
γ_S^{-1}	Average time of symptomatic recovery
γ_A^{-1}	Recovery average time of asymptomatic individuals
γ_H^{-1}	Recovery average time by hospitalization
δ_R^{-1}	Natural immunity
δ_H	Infected symptomatic hospitalization rate

Table 1: Parameters definition of model in Equation (1).

2.1. Parameter calibration

We calibrate parameters of our base dynamics (1) via Multichain Montecarlo (MCMC). To this end, we assume that the cumulative incidence of new infected symptomatic cases CI_S follows a Poisson distribution with mean $\lambda_t = IC_s(t)$. Further, following ideas from [9] we postulate priors for p and κ and count the commulative reported-confirmed cases in the CDMX-Valle de Mexico database [10]

$$\begin{aligned}
 Y_t &\sim \text{Poisson}(\lambda_t), \\
 \lambda_t &= \int_0^t p \delta_E E, \\
 p &\sim \text{Uniform}(0.3, 0.8), \\
 \kappa &\sim \text{Gamma}(10, 50).
 \end{aligned} \tag{2}$$

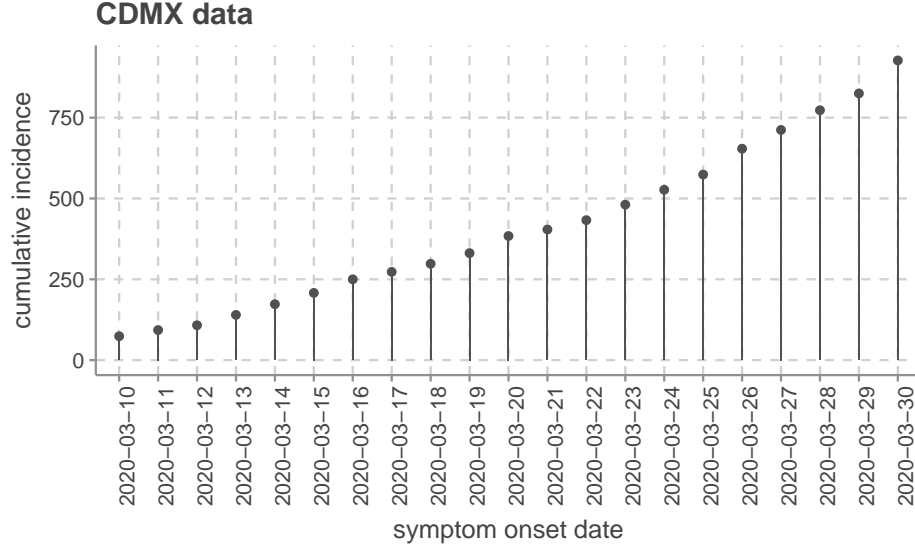


Figure 3: Cumulative new symptomatic and confirmed COVID19 reported cases from Ciudad de Mexico and Valle de Mexico [?] between March, 10, to March 30 of 2020. <https://plotly.com/AdrianSalcedo/48/>

Using Van den Driessche's [11] definition of reproductive number we obtain

$$R_0 := \frac{\kappa}{(\kappa + \mu)(\delta_L + \mu)} (\mu R_1 + \delta_L) \left[\frac{p\beta_S}{R_2} + \frac{(1-p)\beta_A}{\gamma_A + \mu} \right],$$

where

$$R_1 = 1 - \theta(1 - \epsilon),$$

$$R_2 = \mu + \delta_H + \gamma_S + \mu_{I_S}.$$

Figure 3 displays data of cumulative confirmed cases of COVID-19 in Mexico city, and Figure 4 displays the fitted curve of our model in Equations (1) and (2). Table 2 encloses estimated parameters to this setting.

Parameter	Median	Reference
q_r, ϵ	0.4, 0.3, 0.1	***
β_S	$q_r \times 8.690\,483 \times 10^{-1}$	***
β_A	$q_r \times 7.738\,431 \times 10^{-1}$	***
κ	0.196\,078\,43	*
p	0.1213	*
θ	0.2,	this study
δ_L	0.04	postulated
δ_H	0.2	*
δ_V	0.002\,739\,726\,027\,397\,260\,3	Assumed ($\delta_V^{-1} = 2$ years)
δ_R	0.005\,555\,56	Assumed($\delta_R^{-1} \approx 180$ days)
μ	$3.913\,894 \times 10^{-5}$	*
μ_{I_S}	0.0004	*
μ_H	0.016\,32	[12]
γ_S	0.092\,506\,94	*
γ_A	0.167\,504\,19	*
γ_H	$5.079\,869 \times 10^{-1}$	*
λ_V	0.000\,611\,35	Assumed
ε	0.7, 0.9, 0.95	[13–15]
N	26\,446\,435	[16]
L_0	0.266\,260\,097\,021\,127\,96	**
S_0	0.463\,606\,046\,009\,872	**
E_0	0.000\,670\,33	**
I_{S_0}	9.283×10^{-5}	**
I_{A_0}	0.001\,209\,86	**
H_0	$1.341\,579\,69 \times 10^{-4}$	**
R_0	$2.661\,259\,39 \times 10^{-1}$	**
D_0	0.001\,900\,74	**
X_{vac}^0	0.0	***
V_0	0.0	***
$Y_{I_S}^0$	0.122\,581\,64	**
B	0.000\,359\,216\,658\,124\,242\,5	9500 beds/ N
a_{I_S}	0.002\,012\,775\,543\,825\,648\,6	*
a_H	0.001\,411\,888\,738\,103\,725,	*
a_D	7.25	*

Table 2: Model parameters. (*) Values based mainly in [12, 17]. (**) Estimated. (***) This study. (★) From [18].

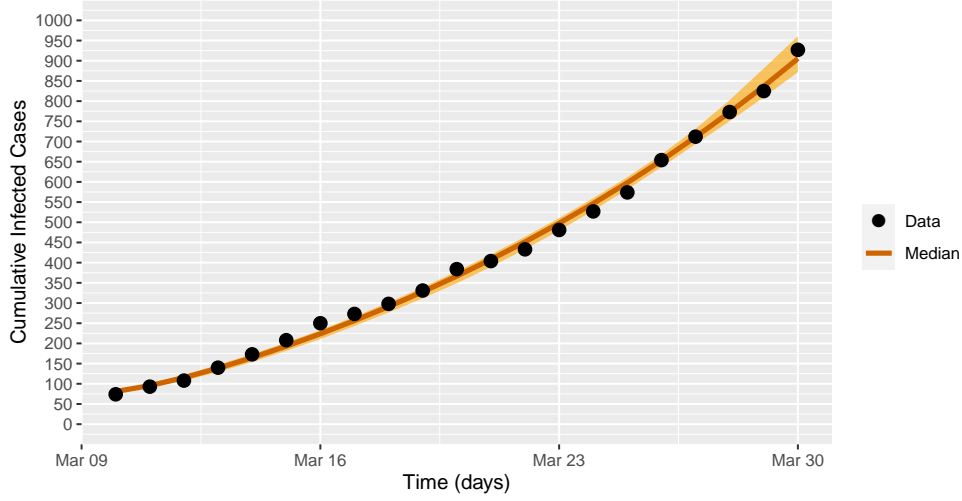


Figure 4: Fit of daily new cases of Mexico city during exponential growth. [https://plotly.com/ AdrianSalcedo/50/](https://plotly.com/AdrianSalcedo/50/)

3. Imperfect-preventive COVID-19 vaccination

The reinfection process on COVID-19 disease at the date of writing this manuscript remains under development. However, our simulations assume reinfection as possible. Thus, $1/\delta_R$ denote the period of natural immunity. Also we assume that the underlying vaccine induces immunity that last 2years. Further, we take vaccine parameters conforming to Pfizer-BioNTech and Aztra-Zeneca developments. Above other important modeling assumptions.

Assumptions 2. According to COVID-19 dynamics in model in Equation (1), we made the following modeling hypotheses about the regarding vaccine.

(VH-1) Vaccine is preventive and only reduce susceptibility.

(VH-2) The vaccination campaign omits testing to detect seroprevalence. Thus Exposed, Infected Asymptomatic and Recovered Asymptomatic individuals are undetected but would obtain a vaccine dose—which in these model represent a waste of resources

(VH-3) Individuals under Lockdown also would be vaccinated

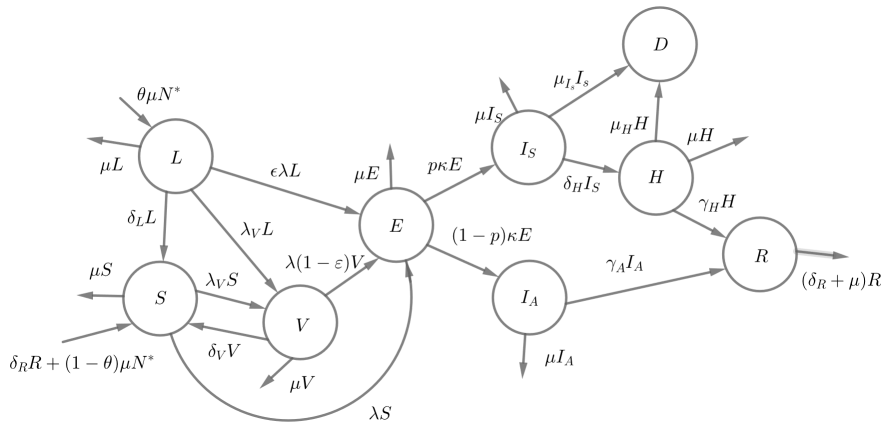


Figure 5: Flux diagram for lockdown-vaccination COVID-19 dynamics.

104 (VH-4) The vaccine is leaky and with efficacy $\epsilon \in [0.7, .975]$

105 (VH-5) Vaccine induced immunity last 2 years

106 (VH-6) Natural immunity last a period of 180 days

According to the spread COVID19 dynamics in Equation (1), we add the compartments L and V to denote the Lockdown and Vaccinated population fractions. Thus, we understand the lockdown intervention as flux between the Lockdown and Susceptible compartmental with rate δ_L . Because around 30% of the population under risk enclose the children and young with scholar age, we assume that a fraction of the susceptible population in Equation (1) is under lockdown but in constant flux with susceptible compartment thus, we formulate the equations

$$\begin{aligned} L' &= \theta \mu N^* - (\epsilon \lambda + \delta_L + \lambda_V + \mu) L \\ S' &= (1 - \theta) \mu N^* + \delta_L L + \delta_V V + \delta_R R \\ &\quad - (\lambda + \lambda_V + \mu) S. \end{aligned}$$

Since our formulation considers a preventive leaky vaccine we add an output from lockdown and susceptible compartments by vaccination with rate λ_V and add the equation

$$V' = \lambda_V (S + L) - [(1 - \epsilon) \lambda + \delta_V + \mu] V.$$

to describe the dynamics of fraction vaccinated population. Also we add the equations

$$\begin{aligned} \frac{dX_{vac}}{dt} &= (u_V(t) + \lambda_V) [L + S + E + I_A + R] \\ \frac{dY_{I_S}}{dt} &= p \kappa E \end{aligned}$$

107 to account the vaccine coverage and incidence.

Then we establish the following ordinary differential equation see Figure 5 and Table 1.

$$\begin{aligned}
L' &= \theta \mu N^* - (\epsilon \lambda + \delta_L + \lambda_V + \mu) L \\
S' &= (1 - \theta) \mu N^* + \delta_L L + \delta_V V + \delta_R R \\
&\quad - (\lambda + \lambda_V + \mu) S \\
E' &= \lambda (\epsilon L + (1 - \epsilon) V + S) - (\kappa + \mu) E \\
I_S' &= p \kappa E - (\delta_H + \gamma_S + \mu_{I_S} + \mu) I_S \\
I_A' &= (1 - p) \kappa E - (\gamma_A + \mu) I_A \\
H' &= \delta_H I_S - (\gamma_H + \mu_H + \mu) H \\
R' &= \gamma_S I_S + \gamma_A I_A + \gamma_H H - (\delta_R + \mu) R \\
D' &= \mu_{I_S} I_S + \mu_H H \\
V' &= \lambda_V (S + L) - [(1 - \epsilon) \lambda + \delta_V + \mu] V
\end{aligned}$$

$$\begin{aligned}
\frac{dX_{vac}}{dt} &= (u_V(t) + \lambda_V) [L + S + E + I_A + R] \\
\frac{dY_{I_S}}{dt} &= p \kappa E \\
\lambda &:= \frac{\beta_A I_A + \beta_S I_S}{N^*}
\end{aligned} \tag{3}$$

$$\begin{aligned}
L(0) &= L_0, \quad S(0) = S_0, \quad E(0) = E_0, \\
I_S(0) &= I_{S_0}, \quad I_A(0) = I_{A_0}, \quad H(0) = H_0, \\
R(0) &= R_0, \quad D(0) = D_0, \\
V(0) &= 0, \quad X_{vac}(0) = 0, \\
X_{vac}(T) &= x_{coverage}, \\
N^*(t) &= L + S + E + I_S + I_A + H + R + V.
\end{aligned}$$

4. Lockdown-Vaccination reproductive number

The basic reproductive number, which is generally denoted by R_0 , is a threshold quantity with which we can use particular control strategies. The epidemiological interpretation of R_0 is the average number of secondary cases produced by an infected individual introduced into a population of susceptible individuals. Using Van DenDrishe's [19] definition of reproductive number we obtain

$$R_0 := \frac{\kappa}{(\kappa + \mu)(\delta_L + \mu)} (\mu R_1 + \delta_L) \left[\frac{p \beta_S}{R_2} + \frac{(1 - p) \beta_A}{\gamma_A + \mu} \right],$$

where

$$\begin{aligned}
R_1 &= 1 - \theta(1 - \epsilon), \\
R_2 &= \mu + \delta_H + \gamma_S + \mu_{I_S}.
\end{aligned}$$

Factor $\frac{p \beta_S}{R_2}$ measures the proportion of new infections generated by a symptomatic infectious individual in the time that it lasts infected. Similarly, factor $\frac{(1 - p) \beta_A}{\gamma_A + \mu}$ measures the new infections generated by an asymptomatic infectious individual. Term $\frac{\mu R_1 + \delta_L}{\delta_L + \mu}$ measures the number of individuals in lockdown that leave the lockdown, which can be infected. And $\frac{\kappa}{\kappa + \mu}$ account the incubation period. If we consider that there is no lockdown, then R_0 results

$$\tilde{R}_0 := \frac{\kappa}{(\kappa + \mu)} \left[\frac{p \beta_S}{R_2} + \frac{(1 - p) \beta_A}{\gamma_A + \mu} \right].$$

Note that we have the relation $R_0 \leq \tilde{R}_0$. These indicate that there is greater transmission of the disease if there is no lockdown. [Here Gabriel's R not calculations.](#)^{SDIV} Considering assumptions 2, we can establish a vaccine reproductive number, in which individuals who have already been vaccinated can become infected individuals by being in contact with the symptomatic infected. Using Van den Driessche's [19] definition of reproductive number and [20], we obtain

$$R_0^V := \left[1 - \frac{\varepsilon \lambda_V}{\mu + \lambda_V + \delta_V} - \frac{\theta \mu (1 - \epsilon)}{\mu + \delta_L + \lambda_V} \right] (\mu R_1 + \delta_L) R_0.$$

The threshold quantity R_0^V is the reproductive number of infection which can be interpreted as the number of infected people produced by one infected individual introduced into the population in the presence of vaccination.

Figure 6, displays the contour curves for R_0^V as function of the efficacy of the vaccine (ϵ) and of the vaccination rate (λ_V), considering an immunity period induced by the vaccine of half year. Orange line, correspond to the values of $\lambda_{V_{base}}$. With this vaccination rate, no matter how effective the vaccine is, it is not possible to reduce the value of R_0^V below one. Black line illustrate a scenario in which we can drive the R_0^V below one, considering a vaccine efficacy of 0.2 and a vaccination rate of 0.7. Here, we stress that lockdown allows the implementation of lower vaccine efficacies to mitigate spread. In contrast Figure 7 displays plausible combinations of ϵ and λ_V values in order to reduce the value of R_V below one. Note that in this case we require vaccine efficacy of 60 % or more and adequate vaccination rate to drive R_0^V below one.

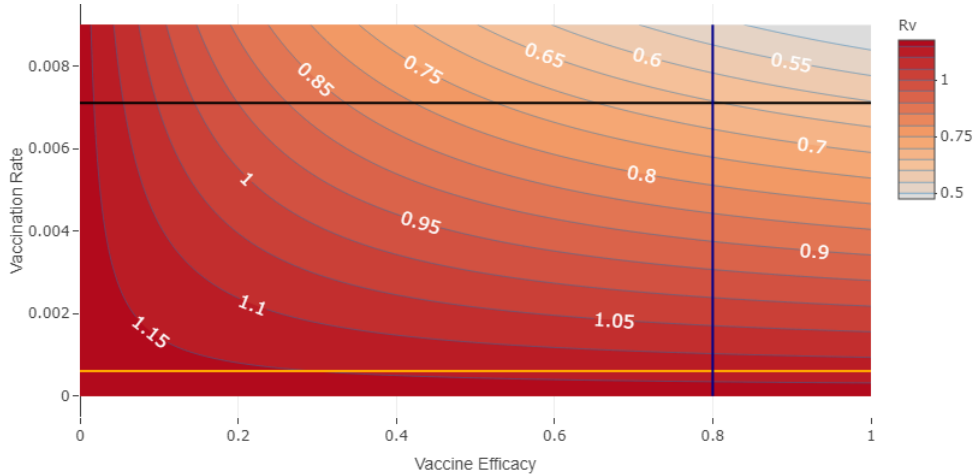


Figure 6: Contour plot of R_0^V as a function of ϵ and λ_V and vaccine-induced immunity average time of half year. orange line represents the value of $\lambda_{V_{base}} = 0.000611$, corresponding to a coverage $x_{coverage} = 0.2$ and a horizon time $T = 365$ days. Intersection of black line and blue line show a scenario in which it is possible to have the $R_V = 0.65$, considering a vaccine efficacy of 0.8 and a vaccination rate of 0.7.

shows the efficacy of the vaccine as a function of the vaccination rate. The blue line, $\varepsilon = 0.8$, tells us what value of λ_V to take for which to have the level curve where $R_0^V < 1$. In the gray region of the figure 7, you can see the values of vaccine efficacy and vaccination rate for which $R_0^V < 1$. In this figure, we consider that the lockdown effect is not present. If we take $\varepsilon = 0.2$, we can see that we always have $R_0^V > 1$ with which choice of λ_V .

In the figure 8, we take into account that the lockdown effect is present. We can see that the gray region, $R_0^V < 1$, is much larger than in the figure. Note that we can choose smaller values for ε and λ_V when we do have an individual lockdown.

[SDIV 3]

Here counts plots figure as function of efficacy and vaccination rate

[1] edit plot range to display level RV=1

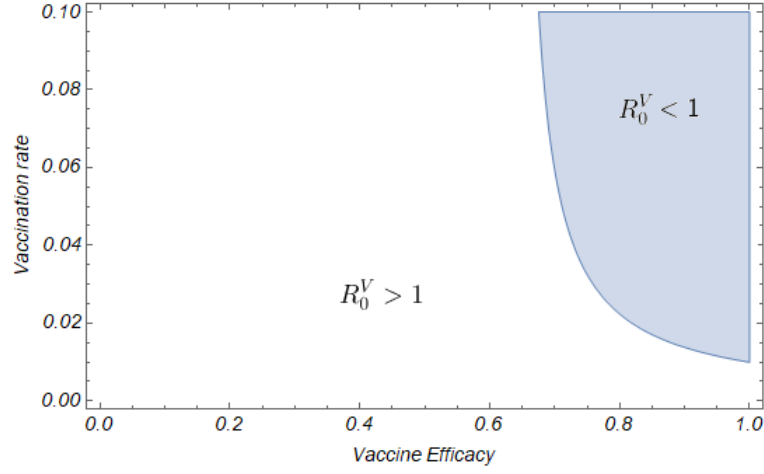


Figure 7: Vaccine efficacy versus vaccination rate feasibility. In the gray shaded region $R_V < 1$ and in the white region $R_V > 1$. Note that, for our scenario, we consider no lockdown individuals. [https://plotly.com/ AdrianSalcedo/52/](https://plotly.com/AdrianSalcedo/52/)

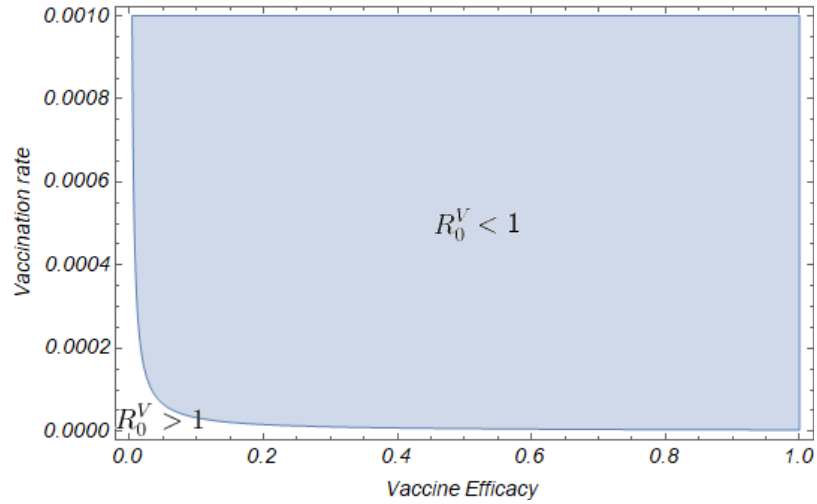


Figure 8: Vaccine efficacy versus vaccination rate feasibility. In the gray shaded region $R_V < 1$ and in the white region $R_V > 1$. Note that, for our scenario, we consider lockdown individuals.

5. Optimal controlled version

Now we model vaccination, treatment and lockdown as an optimal control problem. According to dynamics in Equation (1), we modulate the vaccination rate with a time-dependent control signal $u_V(t)$. We add compartment X_{vac} to count all the vaccine applications of lockdown susceptible, exposed, asymptomatic and recovered individuals. This process is modeled by

$$X'(t) = (\lambda_V + u_V(t))(L + S + E + I_A + R) \quad (4)$$

and describes the number of applied vaccines at time t . Consider

$$x(t) := (L, S, E, I_S, I_A, H, R, D, V, X_{vac})^\top(t)$$

and control signal $u_v(\cdot)$. We quantify the cost and reward of a vaccine strategy policy via the penalization functional

$$J(u_L, u_V) := \int_0^T a_{SP} \kappa E(r) + a_H \delta_H I_S(r) + a_D [\mu_{I_S} I_S(r) + \mu_H H(r)] + \frac{1}{2} [c_L u_L^2(r) + c_V u_V^2(r)] dr. \quad (5)$$

In other words, we assume in functional J that pandemic cost is proportional to the symptomatic hospitalized and death reported cases and that a vaccination and lockdown policies implies quadratic consumption of resources.

Further, since we aim to simulate vaccination policies at different coverage scenarios, we impose the vaccination counter state's final time condition $X_{vac}(T)$

$$\begin{aligned} x(T) &= (\cdot, \cdot, \cdot, \cdot, \cdot, X_{vac}(T))^\top \in \Omega \\ X_{vac}(T) &= x_{coverage}, \\ x_{coverage} &\in \{\text{Low}(0.2), \text{Mid}(0.5), \text{High}(0.8)\}. \end{aligned} \quad (6)$$

Thus, given the time horizon T , we impose that the last fraction of vaccinated populations corresponds to 20%, 50% or 80%, and the rest of final states as free. We also impose the path constraint

$$\Phi(x, t) := H(t) \leq B, \quad \forall t \in [0, T], \quad (7)$$

to ensure that healthcare services will not be overloaded. Here κ denotes hospitalization rate, and B is the load capacity of a health system.

Given a fixed time horizon and vaccine efficiency, we estimate the constant vaccination rate as the solution of

$$x_{coverage} = 1 - \exp(-\lambda_V T). \quad (8)$$

That is, λ_V denotes the constant rate to cover a fraction $x_{coverage}$ in time horizon T . Thus, according to this vaccination rate, we postulate a policy u_v that modulates vaccination rate according to λ_V as a baseline. That is, optimal vaccination amplifies or attenuates the estimated baseline λ_V in an interval $[\lambda_V^{\min}, \lambda_V^{\max}]$ to optimize functional $J(\cdot)$ —minimizing symptomatic, death reported cases and optimizing resources.

Our objective is minimize the cost functional (5)—over an appropriated functional space—subject to the dynamics in equations (1) and (4), boundary conditions, and the path constrain in (7). That is, we search

154 for vaccination policies $u_V(\cdot)$, which solve the following optimal control problem (OCP).

$$\begin{aligned}
\min_{\mathbf{u} \in \mathcal{U}} J(u_L, u_V) &:= \int_0^T a_S p \kappa E(r) + a_H \delta_H I_S(r) + a_D [\mu_{I_S} I_S(r) + \mu_H H(r)] dr + \\
&\quad \int_0^T \frac{1}{2} [c_L u_L^2(r) + c_V u_V^2(r)] dr. \\
\text{s. t.} \\
L' &= \theta \mu N^* - \epsilon \lambda L - u_L(t) L - \mu L \\
S' &= (1 - \theta) \mu N^* + u_L(t) L + \delta_v V + \delta_R R \\
&\quad - [\lambda + (\lambda_V + u_V(t)) + \mu] S \\
E' &= \lambda(\epsilon L + (1 - \epsilon) V + S) - (\kappa + \mu) E \\
I_S' &= p \kappa E - (\gamma_S + \mu_{I_S} + \delta_H + \mu) I_S \\
I_A' &= (1 - p) \kappa E - (\gamma_A + \mu) I_A \\
H' &= \delta_H I_S - (\gamma_H + \mu_H + \mu) H \\
R' &= \gamma_S I_S + \gamma_A I_A + \gamma_H H - (\delta_R + \mu) R \\
D' &= \mu_{I_S} I_S + \mu_H H \\
V' &= (\lambda_V + u_V(t)) S - [(1 - \epsilon) \lambda + \delta_V + \mu] V
\end{aligned} \tag{9}$$

$$\begin{aligned}
\frac{dX_{vac}}{dt} &= (u_V(t) + \lambda_V) [L + S + E + I_A + R] \\
\frac{dY_{I_S}}{dt} &= p \kappa E \\
\lambda &:= \frac{\beta_A I_A + \beta_S I_S}{N^*}
\end{aligned}$$

$$\begin{aligned}
L(0) &= L_0, \quad S(0) = S_0, \quad E(0) = E_0, \quad I_S(0) = I_{S_0}, \\
I_A(0) &= I_{A_0}, \quad H(0) = H_0, \quad R(0) = R_0, \quad D(0) = D_0, \\
V(0) &= 0, \quad X_{vac}(0) = 0, \quad u_V(\cdot) \in [u_{\min}, u^{\max}], \\
X_{vac}(T) &= x_{coverage}, \quad \kappa I_S(t) \leq B, \quad \forall t \in [0, T], \\
N^*(t) &= L + S + E + I_S + I_A + H + R + V
\end{aligned}$$

155 The policies we are considering in the OCP are piecewise constant; see the Appendix for details. OCPs
156 with this class of policies have been studied in different contexts. For instance, a solution method based
157 on the gradient of the cost functional is studied in [21]; convergence results of piecewise constant solu-
158 tions to permanent solutions in linear-quadratic problems are given in [22]; or, in [23], a general numerical
159 methodology to find piecewise constant solutions is proposed. In fact, to find the optimal policies we use
160 the methodology [23]. Even though the existence of solutions to OCPs in the class of piecewise constant
161 policies is known, for completeness, we sketch a straightforward proof in the Appendix under assumptions
162 that hold for the OCP described above.

163 6. Numerical Experiments

164 6.1. Methodology

165 We simulate and scenario corresponding to a hypothetical but plausible initial conditions and parameters.
166 We integrate model in Equation (9) by classic Runge Kutta scheme and solve the optimization stage with
167 the so called Differential Evolution method. Differential Evolution (DE) [24] is an evolutionary algorithm
168 successfully employed for global optimization [25]. The method is designed to optimize functions $f : \mathbb{R}^n \rightarrow \mathbb{R}$.

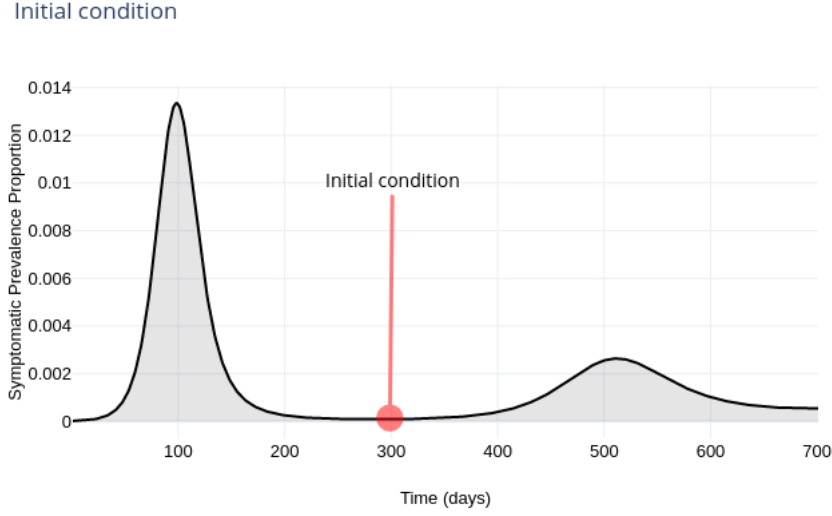


Figure 9: Initial condition scheme. We assume a positive prevalence. Forreference, at the date of write this manuscript, prevalence in CDMX is around 16 000 cases, see <https://plotly.com/sauld/36/> to display a electronic viewer.

Nevertheless, DE can be applied to optimize a functional as stated in [23]. The method can be coded following Algorithm 1, where an initial random population on the search space \mathcal{V} of size N_p is subjected to mutation, crossover and selection. After this process a new population is created which, again would be subjected to the evolutionary process. This process is repeated until some stopping criteria is fulfilled. Finally the best individual (according to some objective function f_{ob} to optimize) is extracted. These operations are conducted by the operators \mathbf{X}_0 , \mathbf{M} , \mathbf{C} , \mathbf{S} , \mathbf{x}_{best} ; whose explicit form are coded in [26].

In the optimization of this study the mutation scale factor F and the crossover probability C_r were taken as 1 and 0.3 respectively, additional N_p has been taken as 4 times the number of parameters (the dimension of the vector used to describe the two controls—see [23]), which in our case was of 180. As stopping criteria we have used a maximum number of generations which is taken as 5000.

We provide in [27] a GitHub repository with all regarding R and Fortran sources for the sake of reproducibility. This repository also encloses data sources and a Wolfrang Mathematica notebook to reproduce all reported figures.

Algorithm 1 Differential Evolution Algorithm

```

 $X \leftarrow \mathbf{X}_0(N_p, \mathcal{V})$ 
while (the stopping criterion has not been met) do
   $M \leftarrow \mathbf{M}(X, F, \mathcal{V})$ 
   $C \leftarrow \mathbf{C}(X, M, C_r)$ 
   $X \leftarrow \mathbf{S}(X, C, f_{ob})$ 
end while
 $\mathbf{x}_{best} \leftarrow \mathbf{Best}(X, f_{ob})$ 

```

181

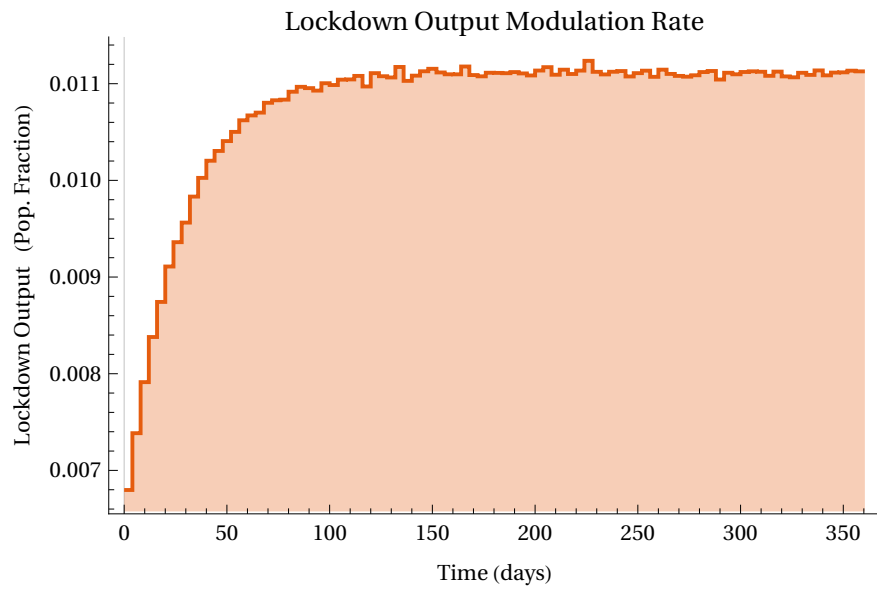


Figure 10: Lockdown modulation signal. [https://plotly.com/ AdrianSalcedo/56/](https://plotly.com/AdrianSalcedo/56/) to display a electronic viewer.

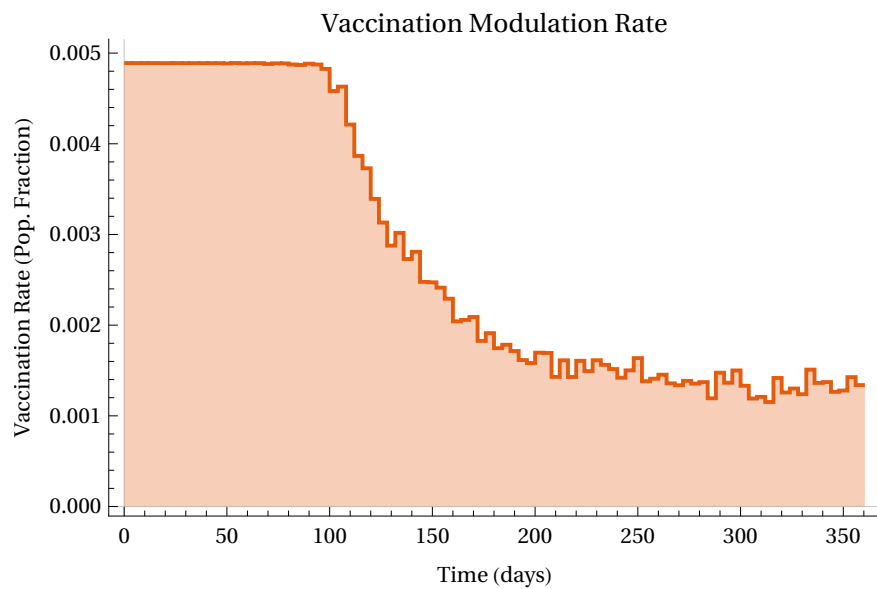


Figure 11: Vaccination rate modulation. [https://plotly.com/ AdrianSalcedo/58/](https://plotly.com/AdrianSalcedo/58/)

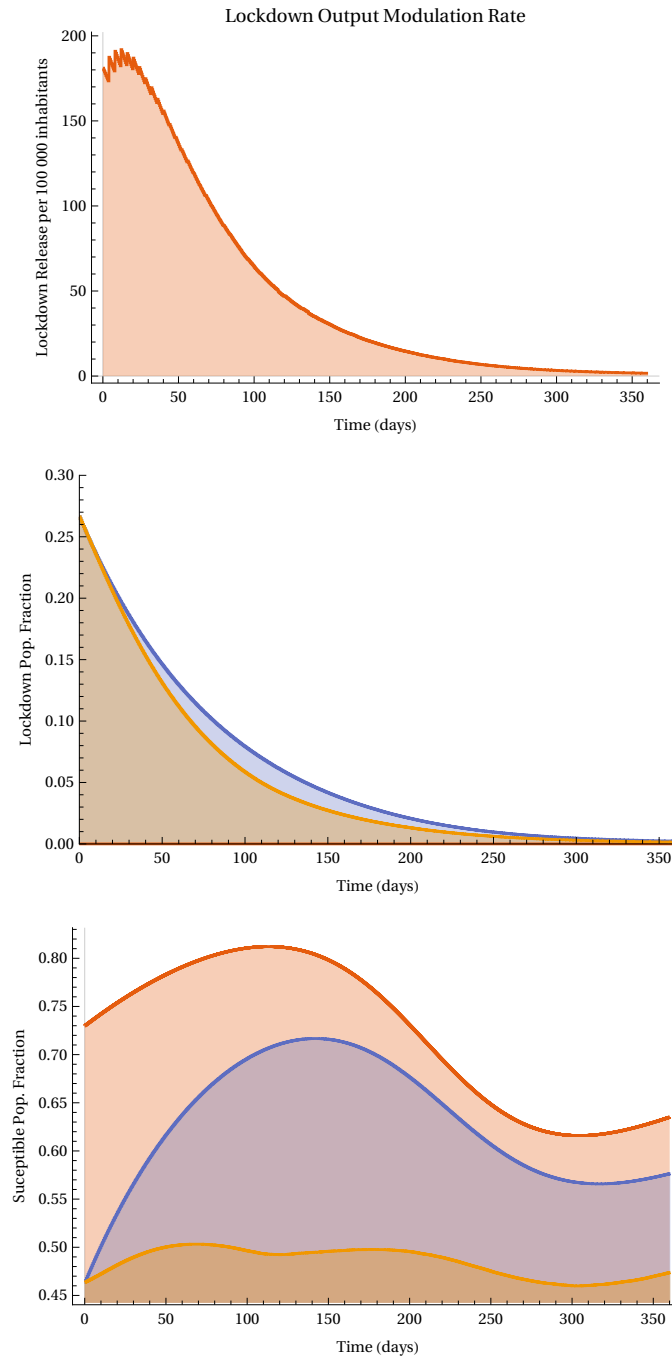


Figure 12: Modulation lock down release. [https://plotly.com/ AdrianSalcedo/60/](https://plotly.com/AdrianSalcedo/60/)

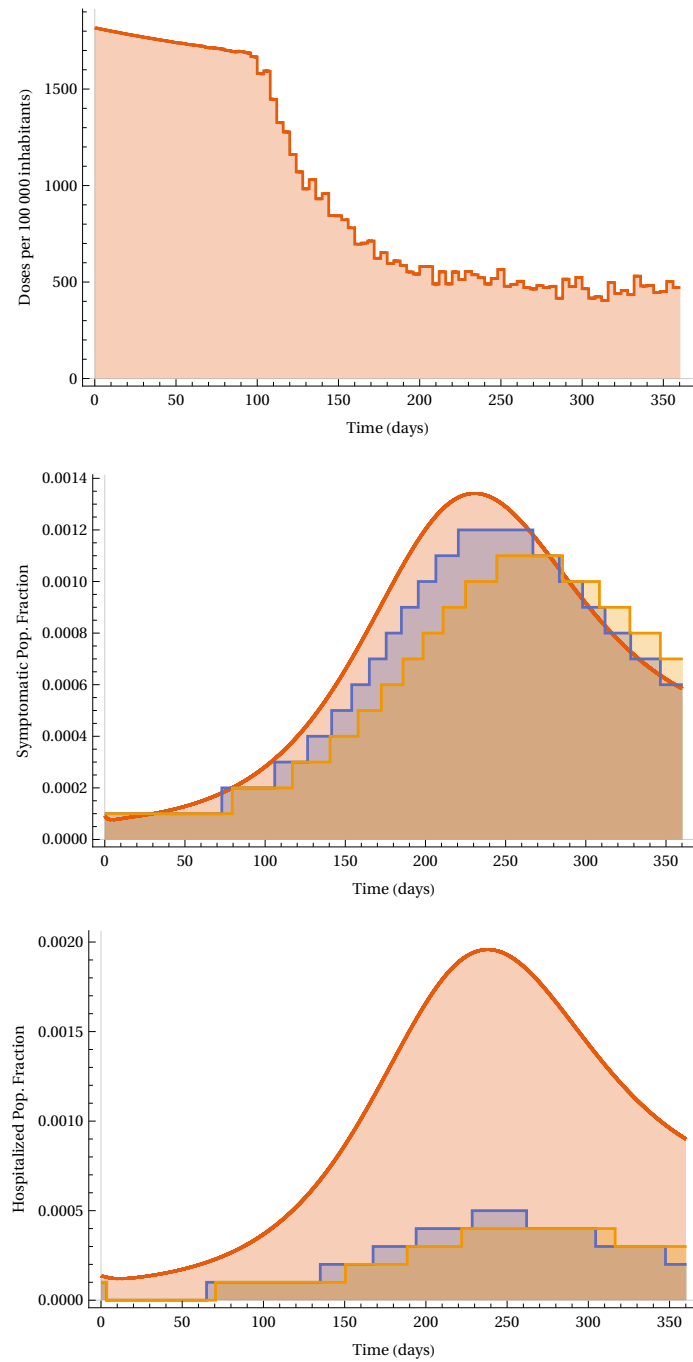


Figure 13: Symptomatic Prevalence and Hospitalization. [https://plotly.com/ AdrianSalcedo/61/](https://plotly.com/AdrianSalcedo/61/)

7. Conclusion

Despite that NPIs has been implemented in most countries to mitigate COVID-19, these strategies can not develop immunity. Thus, vaccination becomes the primary pharmaceutical measure. However, this vaccine has to be effective and well implemented in global vaccination programs, and each development implies particular issues. Thus new challenges in distribution, stocks, politics, vaccination efforts, among others, emerge. In this work, we have studied the effect of the combined strategy lockdown-vaccination and our result suggest that the NPIs would be essential to face the new emergent problems with the accepted vaccines.

We see it very important to implement stratification by risk and age. Thus our efforts will be directed in combination with the result presented in this manuscript.

Data availability

<https://github.com/SaulDiazInfante/NovelCovid19-OptimalPiecewiseControlModelling.git>

Authors' contributions

Gabriel A. Salcedo-Varela Conceptualization, Methodology, Software, Validation, Formal analysis, Investigation, Resources, Visualization, Project Administration, Writing–original draft, Writing–review & editing.

F. Peñuñuri Methodology, Software, Validation, Formal analysis, Investigation, Data curation, Visualization, Supervision, Writing–original draft, Writing–review & editing.

David González-Sánchez: Conceptualization, Methodology, Formal analysis, Writing–original draft, Writing–review & editing.

Saúl Díaz-Infante: Conceptualization, Methodology, Formal analysis, Writing–original draft, Writing–review & editing. Methodology, Software, Validation, Formal analysis, Investigation, Data curation, Visualization, Supervision

Conflicts of interest

The authors have no competing interests.

Appendix A. Existence of optimal policies

In this appendix, we show the existence of optimal policies in the class of *piecewise constant policies*. Consider the following cost functional that we want to minimize

$$\int_0^T C(X(t), u(t)) dt \quad (\text{A.1})$$

subject to the dynamics

$$\dot{X}(t) = f(X(t), u(t)), \quad 0 \leq t \leq T, \quad (\text{A.2})$$

and the initial state $X(0) = x_0$. The functions $u : [0, T] \rightarrow U$ are called *control policies*, where U is a subset of some Euclidean space. Let $t_0 < t_1 < \dots < t_n$, with $t_0 = 0$ and $t_n = T$, be a partition of the interval $[0, T]$. We consider piecewise constant policies \tilde{u} of the form

$$\tilde{u}(t) = a_j \quad t_j \leq t < t_{j+1} \quad (\text{A.3})$$

for $j = 0, \dots, n-1$.

Assumptions 3. We made the following assumptions.

(A-1) The function f in the dynamics (A.2) is of class C^1 .

(A-2) The cost function C in (A.1) is continuous and the set U is compact.

By Assumption (A-1), the system

$$\dot{X}(t) = f(X(t), a_0), \quad X(0) = x_0, \quad 0 \leq t \leq t_1,$$

has a unique solution $\tilde{X}_0(t; x_0, a_0)$ which is continuous in (x_0, a_0) ; see, for instance [28]. Next, put $x_1 := \tilde{X}_0(t_1; x_0, a_0)$ and consider the system

$$\dot{X}(t) = f(X(t), a_1), \quad X(t_1) = x_1, \quad t_1 \leq t \leq t_2,$$

Again, by Assumption (A-1), the latter system has a unique solution $\tilde{X}_1(t; x_1, a_1)$ which is continuous in (x_1, a_1) . By following this procedure, we end up having a recursive solution

$$\begin{aligned} \tilde{X}_{n-1}(t; x_{n-1}, a_{n-1}), \quad t_{n-1} \leq t \leq T, \\ x_{n-1} := \tilde{X}_{n-2}(t_{n-1}; x_{n-2}, a_{n-1}), \end{aligned}$$

where \tilde{X}_{n-1} is continuous in (x_{n-1}, a_{n-1}) .

For a control \tilde{u} of the form (A.3) and the corresponding solution path \tilde{X} , we have

$$\int_0^T C(\tilde{X}(t), \tilde{u}(t)) dt = \sum_{j=0}^{n-1} \int_{t_j}^{t_{j+1}} C(\tilde{X}_j(t), a_j) dt.$$

Notice that each \tilde{X}_j is a continuous function of (a_0, \dots, a_j) and x_0 .

By Assumption (A-2), the mapping

$$(a_0, \dots, a_{n-1}) \mapsto \sum_{j=0}^{n-1} \int_{t_j}^{t_{j+1}} C(\tilde{X}_j(t), a_j) dt$$

is continuous. Since each piecewise constant policy \tilde{u} of the form (A.3) can be identified with the vector (a_0, \dots, a_{n-1}) in the compact set $U \times \dots \times U$, the functional (A.1) attains its minimum in the class of piecewise constant policies.

The cost functional (5) and the dynamics (??) are particular cases of (A.1) and (A.2), respectively, and satisfy Assumptions (A-1) and (A-2). Then there exists an optimal vaccination policy of the form (A.3).

References

- [1] K. M. Bubar, S. M. Kissler, M. Lipsitch, S. Cobey, Y. Grad, D. B. Larremore, Model-informed COVID-19 vaccine prioritization strategies by age and serostatus, medRxiv (2020) 2020.09.08.20190629 (2020).
URL <https://www.medrxiv.org/content/10.1101/2020.09.08.20190629v1>
- [2] L. Matrajt, J. Eaton, T. Leung, E. R. Brown, Vaccine optimization for COVID-19, who to vaccinate first?, medRxiv : the preprint server for health sciences (2020). doi:10.1101/2020.08.14.20175257.
URL <http://www.ncbi.nlm.nih.gov/pubmed/32817963>{%}0Ahttp://www.pubmedcentral.nih.gov/articlerender.fcgi?artid=PMC7430607
- [3] L. Ó. Náraigh, Á. Byrne, Piecewise-constant optimal control strategies for controlling the outbreak of COVID-19 in the Irish population, Mathematical Biosciences 330 (2020) 108496 (dec 2020). doi:10.1016/j.mbs.2020.108496.
URL <https://linkinghub.elsevier.com/retrieve/pii/S0025556420301450>
- [4] S. Ullah, M. A. Khan, Modeling the impact of non-pharmaceutical interventions on the dynamics of novel coronavirus with optimal control analysis with a case study, Chaos, Solitons and Fractals 139 (2020) 110075(1–15) (2020). doi:10.1016/j.chaos.2020.110075.
- [5] M. Mandal, S. Jana, S. K. Nandi, A. Khatua, S. Adak, T. Kar, A model based study on the dynamics of COVID-19: Prediction and control, Chaos, Solitons & Fractals 136 (2020) 109889 (jul 2020). doi:10.1016/j.chaos.2020.109889.
URL <https://doi.org/10.1016/j.chaos.2020.109889><https://linkinghub.elsevier.com/retrieve/pii/S0960077920302897>

- [6] J. S. Weitz, S. J. Beckett, A. R. Coenen, D. Demory, M. Dominguez-Mirazo, J. Dushoff, C. Y. Leung, G. Li, A. Mägälie, S. W. Park, R. Rodriguez-Gonzalez, S. Shivam, C. Y. Zhao, Modeling shield immunity to reduce COVID-19 epidemic spread, *Nature Medicine* 26 (6) (2020) 849–854 (jun 2020). doi:10.1038/s41591-020-0895-3.
URL <https://doi.org/10.1038/s41591-020-0895-3>
- [7] G. B. Libotte, F. S. Lobato, G. M. Platt, A. J. d. S. Neto, Determination of an Optimal Control Strategy for Vaccine Administration in COVID-19 Pandemic Treatment (November 2019) (apr 2020). arXiv:2004.07397.
URL <http://arxiv.org/abs/2004.07397>
- [8] World of Health Organization, WHO methods and data sources for global burden of disease estimates 2000-2011 (Accessed 2020).
URL https://www.who.int/healthinfo/statistics/GlobalDALYmethods_2000_2011.pdf
- [9] M. A. Acuña-Zegarra, M. Santana-Cibrian, J. X. Velasco-Hernandez, Modeling behavioral change and COVID-19 containment in Mexico: A trade-off between lockdown and compliance, *Mathematical Biosciences* 325 (2020) 108370 (2020). doi:10.1016/j.mbs.2020.108370.
- [10] Gobierno de México, Datos abiertos, <https://www.gob.mx/salud/documentos/datos-abiertos-152127> (2020 (Accessed November 10, 2020)).
- [11] P. Van den Driessche, J. Watmough, Reproduction numbers and sub-threshold endemic equilibria for compartmental models of disease transmission, *Mathematical Biosciences* 180 (1-2) (2002) 29–48 (2002). doi:10.1016/S0025-5564(02)00108-6.
- [12] H. Zhao, Z. Feng, Staggered release policies for COVID-19 control: Costs and benefits of relaxing restrictions by age and risk, *Mathematical Biosciences* 326 (2020) 108405 (aug 2020). doi:10.1016/j.mbs.2020.108405.
- [13] N. Kounang, Pfizer says early analysis shows its Covid-19 vaccine is more than 90% effective, prees release (2020).
URL <https://edition.cnn.com/2020/11/09/health/pfizer-covid-19-vaccine-effective/index.html>
- [14] P. Ivanova, Russia says its sputnik v covid-19 vaccine is 92% effective, prees release, November 11, 2020 (2020).
URL <https://www.reuters.com/article/health-coronavirus-russia-vaccine/russia-says-its-sputnik-v-covid-19-vaccine-is-92->
- [15] E. Cohen, Moderna's coronavirus vaccine is 94.5% effective, according to company data, prees release updated November 16, 2020 (2020).
URL <https://edition.cnn.com/2020/11/16/health/moderna-vaccine-results-coronavirus/index.html>
- [16] Comisión Nacional de Vivienda, Proyecciones de población (Accessed November 2020).
URL <https://sniiiv.conavi.gob.mx/demanda/poblacion/proyecciones.aspx>
- [17] N. M. Ferguson, D. Laydon, G. Nedjati-gilani, N. Imai, K. Ainslie, M. Baguelin, S. Bhatia, A. Boonyasiri, Z. Cucunubá, G. Cuomo-dannenburg, A. Dighe, H. Fu, K. Gaythorpe, W. Green, A. Hamlet, W. Hinsley, L. C. Okell, S. Van, H. Thompson, R. Verity, E. Volz, H. Wang, Y. Wang, P. G. T. Walker, C. Walters, P. Winskill, C. Whittaker, C. A. Donnelly, S. Riley, A. C. Ghani, Impact of non-pharmaceutical interventions (NPIs) to reduce COVID- 19 mortality and healthcare demand (March) (2020). doi:<https://doi.org/10.25561/77482>.
- [18] M.-W. Jo, D.-S. Go, R. Kim, S. W. Lee, M. Ock, Y.-E. Kim, I.-H. Oh, S.-J. Yoon, H. Park, The Burden of Disease due to COVID-19 in Korea Using Disability-Adjusted Life Years, *Journal of Korean Medical Science* 35 (21) (2020) e199 (1–10) (2020). doi:10.3346/jkms.2020.35.e199.
- [19] P. van den Driessche, Reproduction numbers of infectious disease models, *Infectious Disease Modelling* 2 (3) (2017) 288–303 (aug 2017). doi:10.1016/j.idm.2017.06.002.
URL <http://dx.doi.org/10.1016/j.idm.2017.06.002https://linkinghub.elsevier.com/retrieve/pii/S2468042717300209>
- [20] M. E. Alexander, C. Bowman, S. M. Moghadas, R. Summers, A. B. Gumel, B. M. Sahai, A vaccination model for transmission dynamics of influenza, *SIAM Journal on Applied Dynamical Systems* 3 (4) (2004) 503–524 (2004). doi:10.1137/030600370.
- [21] K. R. Aida-zade, Y. R. Ashrafova, Optimal control of sources on some classes of functions, *Optimization* 63 (7) (2014) 1135–1152 (2014). doi:10.1080/02331934.2012.711831.
URL <https://doi.org/10.1080/02331934.2012.711831>
- [22] L. Bourdin, E. Trélat, Linear-quadratic optimal sampled-data control problems: convergence result and Riccati theory, *Automatica J. IFAC* 79 (2017) 273–281 (2017). doi:10.1016/j.automatica.2017.02.013.
URL <https://doi.org/10.1016/j.automatica.2017.02.013>
- [23] K. Cantún-Avila, D. González-Sánchez, S. Díaz-Infante, F. Peñuñuri, Optimizing functionals using differential evolution, *Engineering Applications of Artificial Intelligence* 97 (2021) 104086 (2021). doi:<https://doi.org/10.1016/j.engappai.2020.104086>.
- [24] R. Storn, K. Price, Differential evolution – a simple and efficient heuristic for global optimization over continuous spaces, *Journal of Global Optimization* 11 (4) (1997) 341–352 (1997). doi:<https://doi.org/10.1023/A:1008202821328>.
- [25] Bilal, M. Pant, H. Zaheer, L. Garcia-Hernandez, A. Abraham, Differential evolution: A review of more than two decades of research, *Engineering Applications of Artificial Intelligence* 90 (2020) 103479 (2020). doi:<https://doi.org/10.1016/j.engappai.2020.103479>.
- [26] F. Peñuñuri, C. Cab, O. Carvente, M. Zambrano-Arjona, J. Tapia, A study of the classical differential evolution control parameters, *Swarm and Evolutionary Computation* 26 (2016) 86 – 96 (2016). doi:<https://doi.org/10.1016/j.swevo.2015.08.003>.
- [27] S. Diaz-Infante, F. Peñuñuri, D. Gonzalez-Sanchez, G. Salcedo-Varela, Source code for the manuscript Optimal Vaccine Policies for COVID-19 (2020).
URL <https://github.com/SaulDiazInfante/NovelCovid19-OptimalPiecewiseControlModelling.git>
- [28] Q. Kong, A short course in ordinary differential equations, Universitext, Springer, Cham, 2014 (2014). doi:10.1007/

313 978-3-319-11239-8.
314 URL <https://doi.org/10.1007/978-3-319-11239-8>